Sol-gel condensation of rapidly hydrolyzed silicon alkoxides: A joint ^{29}Si NMR and small-angle x-ray scattering study

F. Devreux, J. P. Boilot, and F. Chaput
Laboratoire de Physique de la Matière Condensée, Ecole Polytechnique, 91128 Palaiseau CEDEX, France

A. Lecomte
Ecole Nationale Supérieure de Céramique Industrielle, 87065 Limoges CEDEX, France
(Received 27 December 1989)

We have studied by ^{29}Si NMR the complete condensation kinetics in the conditions of rapid hydrolysis (acidic medium, water in excess) of three silicon alkoxides. The gelation of the tetravalent tetraethoxysilane (TEOS) takes several weeks, whereas the trivalent methyltriethoxysilane (MTEOS) and vinyltriethoxysilane (VTEOS) do not form gels. From a quantitative analysis of the data, we deduce that the first steps of the condensation proceed by progressive assembling of small organized units. This accounts for the very slow kinetics (logarithmic function of time), the occurrence of highly condensed agglomerates, and the absence of gelation in trivalent systems. For the tetravalent TEOS, this is followed by an aggregation phase, which has been studied both by NMR and small-angle x-ray scattering. The fractal dimension $D=1.9$ and the growing kinetics (cluster size increasing as a linear function of time) are consistent with reaction-limited cluster-cluster aggregation with preferential reactivity at the external cluster sites. Finally, we suggest that the progressive transformation of the sol phase into the gel phase after the gel time can be observed by comparing static and magic-angle-spinning NMR spectra.

INTRODUCTION

In addition to its possible interest for the preparation of homogeneous glasses and ceramics, sol-gel condensation of silicon alkoxides offers the unique possibility to build in a more or less controlled way randomized objects, which are believed to be a physical realization of fractal geometry.[1] Moreover, it seems possible to vary the geometry by changing the chemical conditions of the hydrolysis-condensation process.[2] In this respect, there are two key factors: the *p*H, which arbitrates between hydrolysis and condensation rates and the water-to-alkoxide ratio, which governs the hydrolysis level. In the present paper, we are concerned with rapid and nearly complete hydrolysis, which can be achieved by using acidic conditions and excess water. This allows one to separate properly the condensation from the initial hydrolysis. As a counterpart, the condensation can be very slow and the gelation time very long.

Three silicon alkoxides have been used: the well-known tetraethoxysilane [$Si(OC_2H_5)_4$ or TEOS] to which a large number of studies have been already devoted and two new systems having three instead of four branching possibilities, methyltriethoxysilane [$CH_3Si(OC_2H_5)_3$ or MTEOS] and vinyltriethoxysilane [$CH_2CHSi(OC_2H_5)_3$ or VTEOS]. Although these two systems do not form gels, at least in our standard operative conditions, their kinetics are quite similar to that of TEOS in the beginning of the condensation. In some respects, they can be considered as model systems, which allow a better understanding of the complex condensation-aggregation-gelation process by isolation of its first stage.

In the study of sol-gel polymerization of silica, two techniques are mainly used: nuclear magnetic resonance (NMR) provides chemical information at the atomic scale on the initial stages of the hydrolysis and condensation,[3-14] whereas small-angle radiation scattering characterizes the geometrical arrangement in the 1–1000-nm range at the final stage of the process.[15-20] In the present paper, we show that ^{29}Si NMR can be used profitably in the whole condensation process and may provide quantitative information on polymerization kinetics. This requires one to be aware of nuclear relaxation effects, to use magic angle spinning (MAS) in the gel state and, of course, to avoid any silicon-based materials in the NMR probes. In concert with some small-angle x-ray scattering (SAXS) experiments, these data lead us to distinguish three phases in the complex sol-gel condensation of silicon alkoxides: formation of small units, growing of aggregates from these small nits, and finally gelation.

NMR KINETICS

In our experiments, the polymerization process was initiated by adding acidic water to a solution of alkoxide and ethanol. The chemical conditions (water in excess, acidic medium) were chosen in such a way that nearly complete hydrolysis of the alkoxides occurs in a few minutes:

$$Si(OC_2H_5)_4+4H_2O\rightarrow Si(OH)_4+4C_2H_5OH$$

$$R\text{—}Si(OC_2H_5)_3+3H_2O\rightarrow R\text{—}Si(OH)_3+3C_2H_5OH$$

where $R=CH_3,C_2H_3$. This allows to study separately the condensation kinetics which result from the forma-

TABLE I. ^{29}Si chemical shifts (in ppm with respect to TMS) of the three precursors $CH_3Si(OC_2H_5)_3$ or MTEOS, $CH_2CHSi(OC_2H_5)_3$ or VTEOS, and $Si(OC_2H_5)_4$ or TEOS and of the fully hydrolyzed derived Q^i species.

	Precursor	Q^0	Q^1	Q^2	Q^3	Q^4
MTEOS	−42.5	−37.5	−46.7	−56	−65	
VTEOS	−57.5	−52.7	−61.9	−71	−80	
TEOS	−82.0	−72.1	−81.5	−91	−100	−109

tion of siloxane bridges between the hydrolyzed species:

$$\equiv SiOH + \equiv SiOH \rightarrow \equiv Si—O—Si\equiv + H_2O\ .$$

In acidic medium, this condensation process is very slow and the gelation, when it occurs, may require several weeks. Some experiments have been also carried out in basic conditions for comparison.

Figure 1 shows typical ^{29}Si NMR spectra as a function of time for MTEOS, VTEOS, and TEOS systems. The alkoxide:ethanol:water concentration ratios were 1:6:10 and the *p*H of the added water solution was fixed to 2.5 by addition of 13.3 g/ℓ of chromium nitrate $Cr(NO_3)_3 \cdot 9H_2O$. This corresponds to a concentration of 8×10^{-3} mol/ℓ of paramagnetic centers in the polymerization solution. Chromium nitrate was chosen to enhance the ^{29}Si relaxation instead of the usual chromium acetyl-acetonate, so as to avoid a possible drift in the acidity of the solution by progressive chemical evolution of the later complex during the lengthy polymerization. The samples were kept at a constant temperature of 21 °C throughout the experiment. NMR spectra were recorded at 71.54 MHz with a BRUKER MSL 360 spectrometer, using a homemade silicon-free probe for the liquid state and a Doty magic-angle-spinning (MAS) probe for the gel state. Each spectrum corresponds to 360 accumulations. The repetition time was chosen as a compromise between nuclear relaxation and kinetics: long enough to allow nuclear magnetization recovery, short enough to avoid excessive averaging of the kinetics. We take it as 1 s during the first three hours (1 spectrum every 6 min) and then 10 s (1 spectrum per hour). Kinetics were followed continuously during the first day and occasionally afterwards.

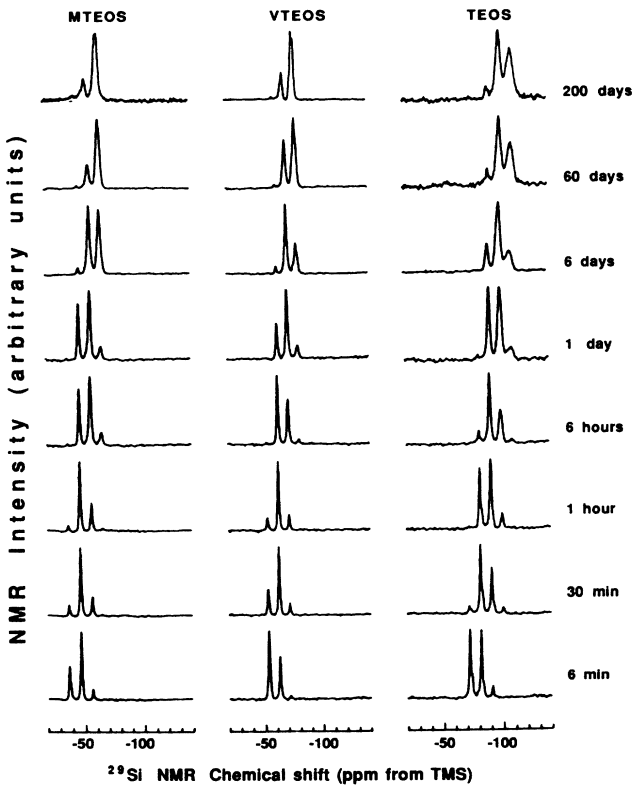

FIG. 1. ^{29}Si NMR spectra at different times during the condensation of MTEOS, VTEOS, and TEOS. The last two spectra for TEOS which correspond to the gel state have been obtained using magic angle spinning.

The data in Fig. 1 have been obtained with a field resolution of about 1 ppm. Although this is not enough to distinguish subtle details in the molecular structure as in high resolution studies,[3-14] this is quite sufficient to separate and to evaluate quantitavely the relative contributions of the silicon atoms with 0, 1, 2, 3, or 4 siloxane bridges, which are conventionally denoted as Q^0, Q^1, Q^2, Q^3, or Q^4. The values of the chemical shifts (in reference to tetramethylsilane or TMS) of these various species are listed in Table I. The beginning of the TEOS condensation has been also recorded with a better resolution (0.2 ppm). These improved resolution data are shown in Fig. 2. They allow us to distinguish different sorts of Q^0, Q^1, Q^2 species and to a smaller extent different sorts of Q^3 species. For MTEOS and VTEOS, the hydrolysis is almost completed within the time necessary to record the first spectrum, that is about 10 min (time to mix the solutions, set up the probe and record the data). For TEOS, a small fraction (less than 10%) of species with one nonsubstituted OR may remain after an hour. This quasi-absence of partially hydrolyzed species leads to quite simple spectra, which could submit accurately to quantitative analysis.

The complete evolution is quantified in Fig. 3, which displays the relative concentration q_i of the Q^i species as a function of the logarithm of the time. Also shown is the evolution of the degree of condensation defined as $c = \sum_i iq_i/f$, with f being the connectivity of the monomer ($f=3$ for MTEOS and VTEOS and $f=4$ for TEOS). This degree of condensation characterizes the progress of the condensation reactions as a whole. The hydrolyzed monomers (Q^0) disappear within one or two hours and the end species (Q^1) in one day for TEOS and one week for MTEOS and VTEOS. A few hours is also the time required for the onset of the most condensed species (Q^3 for MTEOS and VTEOS, Q^3 and Q^4 for TEOS). Gelation

does not occur for MTEOS and VTEOS and takes 1200 h for TEOS. A noteworthy feature in Fig. 3 is that the degree of condensation increases as the logarithm of the time in a large part of the kinetics: almost up to the saturation for the trivalent MTEOS and VTEOS and up to $c \approx 0.6$ for TEOS.

It was checked that the spectrum area was constant within 15%, which means that no significant part of the ^{29}Si signal was missed throughout the condensation process. To establish this point firmly, we have performed relaxation measurements at different stages of the TEOS evolution. The ^{29}Si relaxation is controlled by the dipolar coupling with the mobile chromium paramagnetic ions, whose concentration is fixed (8×10^{-3} mol/l). Before adding water, a solution of TEOS and ethanol with the same chromium concentration has a ^{29}Si relaxation time of 12 s. Immediately after the addition of water, it decreases to about 0.5 s and then increases to 1 s at the end of two hours. These two figures are only a rough estimate, because it is quite impossible to perform accurate relaxation measurements on rapidly evolving spectra. The main reason for the initial enhancement of the relaxation is the replacement of the bulky alkyl radicals by the small hydroxyl groups, which allows a closer contact between Si nuclei and chromium spins, giving rise to a much larger effective dipolar coupling. As the condensation takes place, the opposite effect is expected. However, it is counterbalanced by the growth of the agglomerates, which should enhance the solution viscosity and thus increase the correlation time for molecular diffusion, resulting in a more efficient relaxation process. One day after the beginning of the reaction, it is possible to get reliable measurements for the different peaks: $T_1 = 2$ and 3 s for Q^2 and Q^3. At $t = 7$ days, one obtains $T_1 = 1.8$, 3.1, and 5.1 s for Q^2, Q^3, and Q^4, respectively and at $t = 51$ days, $T_1 = 3.5$ and 4.6 s for Q^3 and Q^4. It turns out that these values do not change too much during the condensation process and that T_1 is longer for more condensed species, as expected. No drastic change is observed at the gel time t_g, indicating that the microscopic diffusion of the paramagnetic centers does not get frozen. Only at times much longer than t_g, the relaxation becomes nonexponential, pointing out the disappearance of the motional relaxation regime. In any other cases, the measured relaxation rate is generally more than twice the repetition rate used in the kinetics experiments. This is actually sufficient to warrant accurate evaluation of the relative contribution of the different peaks.

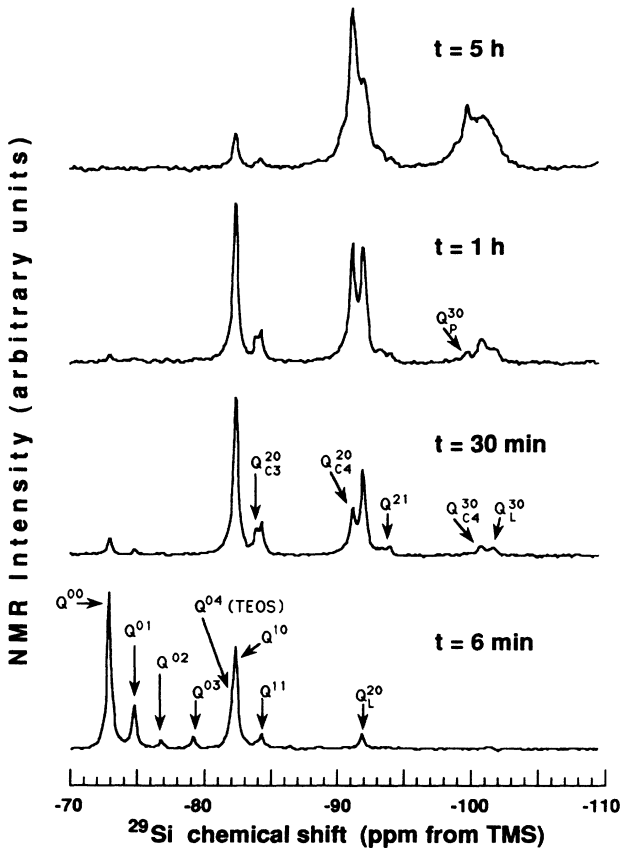

FIG. 2. Detailed ^{29}Si NMR spectra at different times in the beginning of the TEOS condensation. Q^{ij} denotes a silicon atom with i siloxane bondings and j alkyl side groups. Indices L, $C3$, $C4$, P stand for linear, three-membered cycle, four-membered cycle, and polyhedral, respectively.

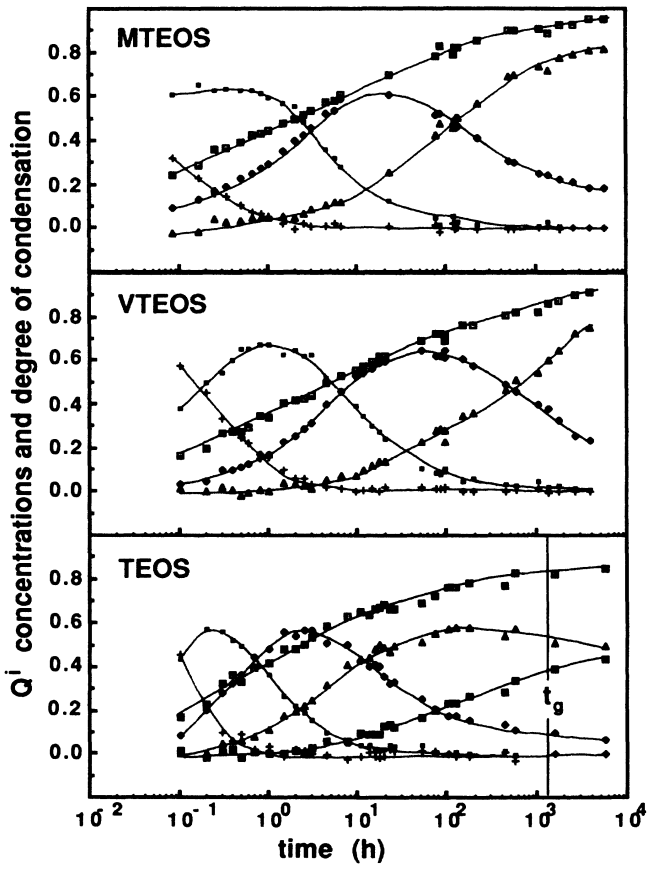

FIG. 3. Time evolution of the concentration of the different Q^i species and of the degree of condensation c for MTEOS, VTEOS, and TEOS (Q^0=cross, Q^1=small square, Q^2=diamond, Q^3=triangle, Q^4=large square, c=open square).

CHEMICAL

Calculations of the paramagnetic shielding of the ^{29}Si nucleus in tetracoordinated silicon compounds show an approximately linear correlation between the relative screening constant and the net charge q on the silicon atom in the $[-40, -120]$ chemical shift range.[21] In that range, increasing the net charge induces a shielding and leads to high-field shift. The position of the resonance peaks for MTEOS, VTEOS, and TEOS (Table I) shows that the presence of nonhydrolyzable radicals (methyl, and to a smaller extent vinyl) causes a down-field shift of the resonance. This corresponds to the inductive effect of the methyl and vinyl radicals which leads to a lowering of the positive charge at the silicon. In the same way, the replacement of an O*R* group by an hydroxyl one during the hydrolysis gives also a down-field shift corresponding to a decrease of q due to a weakening of the effective oxygen electronegativity in the more ionic OH bond. On the opposite, the replacement of one OH group by a siloxane bridge Si—O—Si in the condensation reaction leads to a remarkably constant high-field shift: $\Delta\delta = -9.2 \pm 0.2$ ppm, whatever the precursor and the order of the substitution are (see Table I). This is caused by the increase of the effective oxygen electronegativity from the OH bond to the covalent O—Si bond.

NMR data qualitatively show that the replacement of an O*R* group by nonhydrolyzable radicals leads to higher hydrolysis rates. Actually, in acidic conditions these radicals enhance the electrophilic reactions[22,23] by increasing the negative charge at the oxygen. On the other hand, the presence of vinyl and methyl groups decreases the condensation rate. This can be quantified by the values of $dc/d\log_{10}t$ in the linear part of the curves in Fig. 3, which are, respectively, 0.19, 0.21 and 0.24 for MTEOS, VTEOS, and TEOS. These differences in the condensation reactivity reflect the change in the charge q at the silicon atom, which is the key parameter for the nucleophilic condensation process above the isoelectric point (pH=2).[24–26] An even more pronounced difference was observed in an experiment made using water at pH=5.9: $dc/d\log_{10}t$ was 0.25 and 0.35 for MTEOS and VTEOS, respectively. It would seem that this charge effect may give rise to an increase of the condensation rate as the condensation advances because of the increasing charge at the silicon when going from Q^0 to Q^4. This is actually not observed. On the contrary, the condensation kinetics is slower and slower (logarithmic function of time). As discussed below, this may be explained by the progressive formation of small structured units which involves an increasing bond deformation energy.

Kinetics have been also followed by NMR for various mixtures of MTEOS, VTEOS, and TEOS at different pH. The evolution of the Q^i species is similar to the observed one in pure systems. For example, for a 1:1 mixture of MTEOS and VTEOS with water at pH=5.9, the values of $dc/d\log_{10}t$ (0.31 and 0.33 for MTEOS and VTEOS, respectively) were intermediate between those observed for pure precursors in the same conditions, suggesting intercondensation between the two precursors. Mixing trivalent precursor with TEOS generally inhibits the gelation, except for small percentage of the trivalent component (less than 20%).

In basic conditions, the hydrolysis is controlled by nucleophilic reactions,[22] which are depressed in MTEOS and VTEOS by the decrease of the positive charge at the silicon (due to the inductive effect of the methyl and vinyl radicals). This has been confirmed by an experiment on a 1:1 MTEOS-TEOS mixture with water at pH=10: the hydrolysis is practically inhibited for MTEOS and remains significant, yet slow, for TEOS. Partially hydrolyzed TEOS groups which are observed rapidly condense with other TEOS molecules. No intercondensation is noted in these conditions and the resulting gel is formed only with TEOS components as shown by the ^{29}Si NMR spectrum.

FORMATION OF SMALL UNITS

There are several indications that the beginning of the condensation process in our rapidly hydrolyzed systems corresponds to the formation of small units. First of all, it is seen in Fig. 3 that the degrees of condensation reach very high values: 0.95 without gelation for the trivalent systems and 0.81 at the gel point for TEOS. This indicates highly condensed agglomerates, which are not consistent with a simple random polymerization of monomer units; neglecting intracluster condensation, the maximum value for c would be $2/f$, i.e., 0.67 for MTEOS and VTEOS and 0.5 for TEOS. To explain the observed values of c, it is necessary to assume either that the polymerization involves considerable intracluster condensation at each step or that the primary units which polymerize are already highly condensed objects. As the first explanation is not consistent with the fractal structure observed for the final aggregates (see below), we favor the second one. Actually, if we assume for simplicity that the starting units are uniform and made of n silicon atoms with a degree of condensation c_0, the final degree of condensation will be $c_\infty = c_0 + 2/nf$. In the case $f=4$ (TEOS), this will give the following values for different simple primary units: three-membered cycle ($n=3$),

$$c_0 = \tfrac{1}{2}, \quad c_\infty = \tfrac{2}{3} = 0.67 ,$$

four-membered cycle ($n=4$),

$$c_0 = \tfrac{1}{2}, \quad c_\infty = \tfrac{5}{8} = 0.63 ,$$

eight-membered cube ($n=8$),

$$c_0 = \tfrac{3}{4}, \quad c_\infty = \tfrac{13}{16} = 0.81 .$$

Incidentally, this shows that the cycles are not condensed enough to account for the final degree of condensation in TEOS.

Two kinds of information, structural and kinetic, are contained in Fig. 3. To discard the kinetic ones, one may eliminate the time as a parameter. This is done on Fig. 4, where the q_i's are plotted versus c. The general shape of the resulting curves is remarkable with an almost perfect symmetry with respect to $c=\frac{1}{2}$. It can be compared to two limiting models: random branching and ordered hierarchical arrangement. In the case of entirely random branching, the q_i's should follow the binomial laws:

$$q_i = C_f^i c^i (1-c)^{f-i},$$

where C_f^i is the binomial coefficient. The resulting curves are displayed in the bottom part of Fig. 5 for $f=3$ and 4. The intermediate curves ($i \neq 0, f$) exhibit a maximum at $c = i/f$ with a maximum value around 0.4. On the opposite, for a step-by-step condensation process where each condensation step proceeds more slowly than the preceding one, one expects $q_i = 1$ and $q_{j \neq i} = 0$ when $c = i/f$, that is only dimers when $c = 1/f$, only Q^2 cycles for $c = 2/f$ and only three-dimensional Q^3 boxes for $c = 3/f$. Extrapolated curves between these points would have the triangular shape

$$q_i = \max(0, 1 - |i - fc|)$$

and are shown in the top of Fig. 5.[27] The experimental results on Fig. 4 give a maximum value of $q_{\max} \approx 0.6$, which is intermediate between those obtained for random branching ($q_{\max} \approx 0.4$) and for ordered arrangement ($q_{\max} = 1$). This indicates that the beginning of the condensation is far from being completely random, but rather involves to a certain extent a step-by-step assembly, leading to the formation of presumably small and more or less ordered units.

This conclusion is consistent with the existence of stable polyhedral oligomers with 8 or 10 silicon atoms, which have been previously noticed in the case of MTEOS.[28] Moreover, it is confirmed by the data in Fig. 2, which show the details of the beginning of TEOS condensation. In particular, it is possible to distinguish the different Q^2 species: three-membered cycles at -83.8 ppm, four-membered cycles at -91.1 ppm, and linear chains or larger cycles at -91.8 ppm. The spectra clearly show that the linear Q^2, which first appear as expected, are progressively transformed in quaternary cycles. A weak signal of Q^2 ternary cycles is also present, but it disappears after three or four hours. A similar effect is also apparent for the Q^3 lines. High-field features first appear at -101.7 ppm and then at -100.9 ppm. They correspond to linearly branched Q^3 and to Q^3 belonging to a quarternary cycle, respectively. At the end of one hour, a low field peak begins to grow at -99.7 ppm and becomes dominant after four or five hours. This new peak is probably due to Q^3 silicon inserted in a polyhedral structure involving two or three small cycles (for example a cubic octamer), as it is known that the reduction of the O—Si—O angle, which is expected in such unit, leads to deshielding (down-field shift). These observations are consistent with that of Kelts and Armstrong, who rely on their high-resolution NMR study to emphasize the role

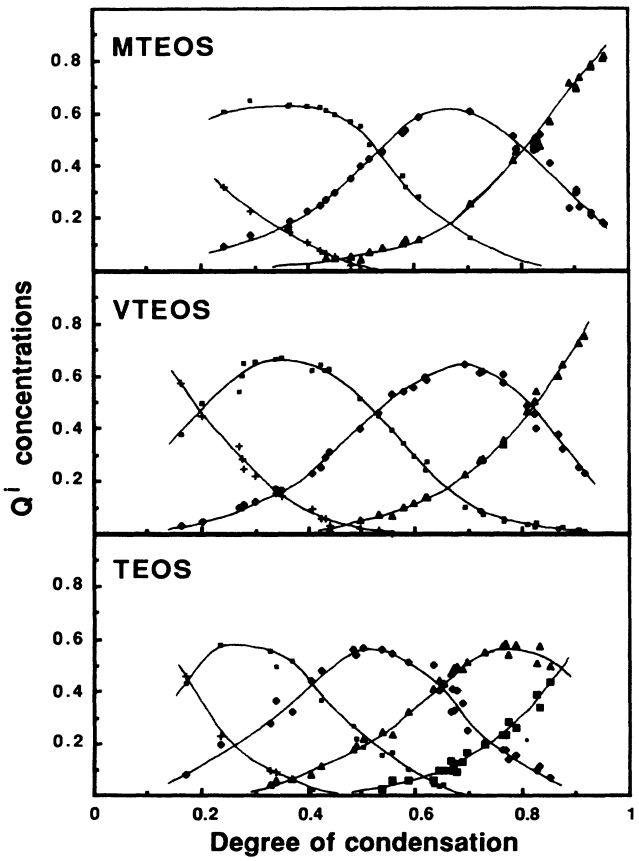

FIG. 4. Concentration of the different Q^i species vs the degree of condensation c for MTEOS, VTEOS, and TEOS (Q^0=cross, Q^1=small square, Q^2=diamond, Q^3=triangle, Q^4=large square).

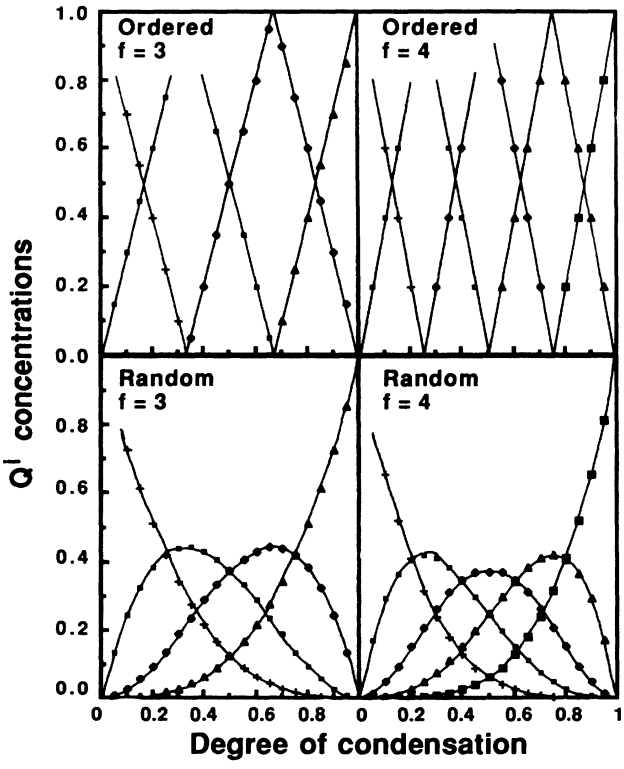

FIG. 5. Theoretical curves for the concentration of the different Q^i species vs the degree of condensation c for $f=3$ and $f=4$ in the cases of random branching and hierarchical ordered arrangement (Q^0=cross, Q^1=small square, Q^2=diamond, Q^3=triangle, Q^4=large square).

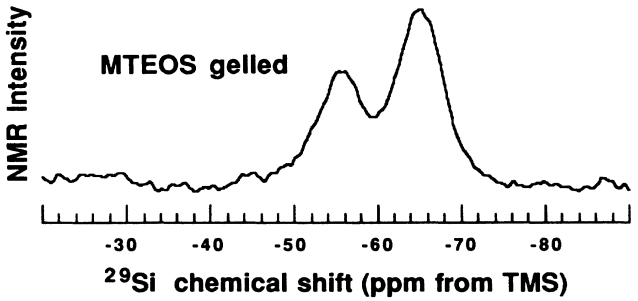

FIG. 6. MAS ^{29}Si NMR spectrum of a MTEOS gel obtained by slow hydrolysis at a hexane-ethanol interface.

of the compact rings in TMOS (tetramethoxysilane) and TEOS condensation.[14]

A further evidence for the formation of small condensed units is the absence of gelation in trivalent compounds, whereas the degree of condensation is as high as 0.95. The MTEOS and VTEOS solutions have been checked by the SAXS technique at the very end of the condensation process. No contrasting intensity was observed, implying a major limit for the size of the particles in the order of 0.7 nm. In fact, to reach the gel state in trivalent systems, it is necessary to inhibit the formation of the small units. This may be done by slowing the hydrolysis with respect to the condensation, in order to prevent the arrangement of the condensed molecules by the presence of nonhydrolyzed side groups. As seen above, this cannot be achieved by using basic catalysis, because the hydrolysis becomes excessively long. However, we have succeeded in causing a MTEOS system to gel by compelling a slow hydrolysis at the interface of a mixture of hexane and MTEOS and a mixture of acidic water and ethanol. In Fig. 6, the ^{29}Si MAS spectrum of the gelled state shows a q_2:q_3 ratio larger than in the last MTEOS spectrum on Fig. 1 (35:65 versus 17:83), which confirms that, to reach gelation, it is necessary to inhibit the formation of excessively condensed units.

Finally, the formation of small units can account for the fact that the degree of condensation increases as a logarithmic function of the time in a large part of the kinetic evolution. This functional dependence is much slower than those usually expected for first- and second-order kinetics, $c \sim 1-\exp(-t)$ and $c \sim t/(1+t)$, respectively. The logarithmic law corresponds rather to a kinetic equation of the form: $dc/dt \sim \exp(-c)$. In fact, such an equation is not unexpected according to the above structural considerations. The mentioned step-by-step condensation would require bond deformations and possible bond breakings and reformings. In any case, this process should involve an energy barrier which is expected to be proportional to the mean number of already formed siloxane bridges per silicon atom: this may explain that the kinetic constant contains a thermally activated term with an activation energy proportional to c.

AGGREGATION

In TEOS, the formation of small units does not prevent further condensation by aggregation of these units in large macromolecules. This is due to the availability of four bonds instead of three, and possibly to the lower hydrolysis rate which may preserve some bonding possibilities for condensation after the formation of the small units. According to the previous discussion, this aggregation stage begins at the end of the logarithmic part of the $c(t)$ curve in Fig. 3(c), that is for $t \approx 1$ day and $c \approx 0.6$. This has been confirmed by SAXS measurements made on a TEOS solution identical to the one studied by NMR, which show that particles of detectable size begin to grow after about one day. The SAXS curves at later times are shown in Fig. 7(a). The scattered intensity $I(K)$ is plotted versus the scattering vector amplitude defined as $K=(4\pi/\lambda)\sin(\theta/2)$, where θ is the total scattering angle

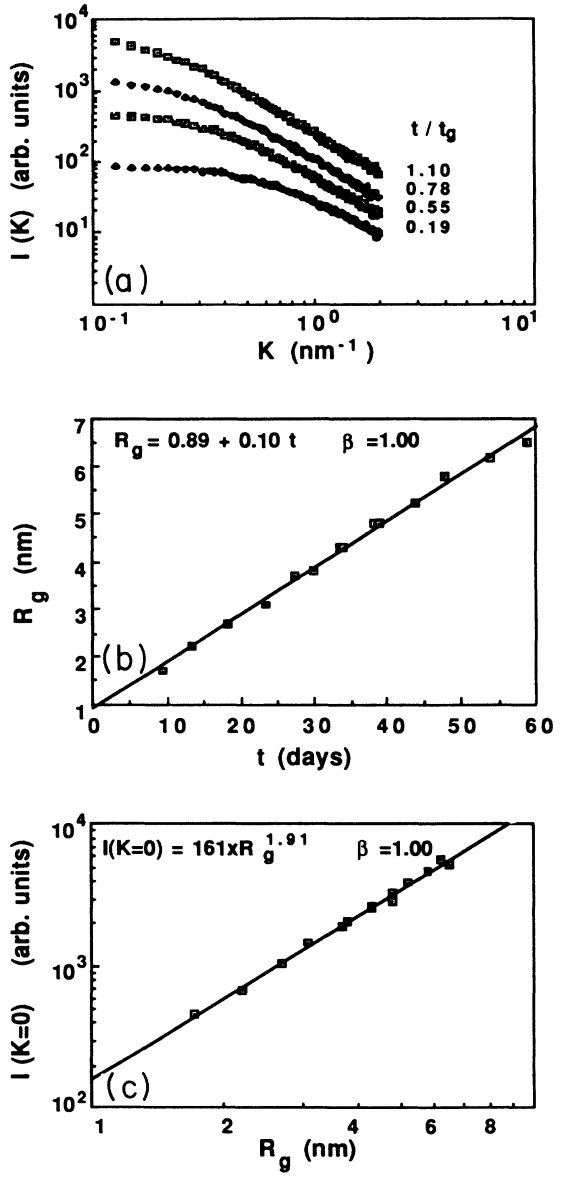

FIG. 7. SAXS data for a TEOS solution during the condensation: (a) scattering curves $I(K)$ at different times; (b) time evolution of the Guinier radius; (c) scaling law $I(K=0) \sim R_g^D$ between the scattered intensity at $K=0$ and the Guinier radius. In (b) and (c) β is the correlation coefficient of the fit.

and λ the wavelength of the incident x-rays. The SAXS data were recorded with a slit type camera (Cu $K\alpha$ wavelength, quartz monochromator). A sample cell was used with 0.025-mm Mylar windows and 0.5–1-mm path length. The sample to detector distance was 500 mm and the scattered intensity was counted with a position-sensitive proportional counter. Experimental results are corrected for parasite scattering and normalized to equivalent sample thickness, incident intensity, and counter efficiency.

Far from the gel point, the radius of gyration R_g of the aggregates can be obtained from a Guinier analysis of these curves.[29] It is shown in Fig. 7(b) that R_g increases linearly with time in a large part of the growing process: $R_g = r_0 + at$, with $r_0 = 0.9$ nm and $a = 0.1$ nm/day. Moreover, assuming mutual self-similarity between the aggregates at different times, it is possible to determine the fractal dimension D: actually, the proportionality of the intensity at wave number $K = 0$ to the mean cluster mass M leads to $I(K=0) \sim M \sim R_g^D$. The scaling law between $I(K=0)$ and the Guinier radius is shown in Fig. 7(c): it gives $D = 1.9$. The volume fraction Φ occupied by the clusters can be deducted from $\Phi = \Phi_i (R_g / r_i)^{3-D}$, with Φ_i and r_i being the initial volume fraction and molecule radius. Taking $\Phi_i = 0.05$ and $r_i = 0.3$ nm for the initial solution of hydrolyzed monomers, it turns out that $\Phi \sim 1$ is obtained for $R_g \sim 5$ nm. It is seen in Fig. 7(b) that this corresponds roughly to the size reached at the gel time $t_g \sim 50$ days. Although significant, this agreement should be considered only as qualitative because, as shown above, the fractal growth begins at the small unit level rather than at the monomer level. Moreover, it should be kept in mind that the previous analysis of the SAXS data breaks down when the spatial correlations between neighboring clusters begin to screen the correlations inside individual clusters. This corresponds precisely to the time at which the volume fraction approaches unity.

Let us now address the question of the kinetics in the aggregation phase. From the time scale involved in this growing process, it is clear that the kinetics is controlled by chemical reaction rather than diffusion. This process is known as reaction-limited cluster aggregation[30] (RLCA) and has been previously proposed by Schaefer and co-workers to describe the acid-catalyzed growth of silicates.[31–33] However, the linear time dependence observed in Fig. 7(b) contrasts with the exponential law expected for this mechanism[34,35] and observed experimentally at larger scale by light scattering in different dilute systems.[20,36] Although this discrepancy can be due to the above-mentioned screening effect, it could be also explained by a slight modification of the RLCA mechanism. Actually, the time dependence of the mass of the cluster

$$M/m_0 = (R/r_0)^D = (1 + at/r_0)^D \quad (1)$$

seems to be nearly quadratic. This would imply a kinetic equation of the form $dM/dt \sim \sqrt{M}$ instead of the usual $dM/dt \sim M$, which gives rise to the exponential growth. Such a behavior could be explained by assuming that the condensation reactions take place preferentially at the external sites of the fractal agglomerates. Then, the kinetic constant should be proportional to the external surface, that is, to $M^{(D-1)/D} \sim \sqrt{M}$. This might be due either to chemical reasons (better reactivity of peripheral sites) or to geometrical ones (steric hindrance of the rigid macromolecules). Such a mechanism would be consistent with the measured fractal dimension $D = 1.9$, which is slightly less than the value $D = 2.1$ corresponding to unrestricted RLCA. It could also account for the rounded mass distribution observed in acid-catalyzed TEOS aggregation,[37,38] which contrasts with the power-law distribution expected in the RLCA mechanism.[31,32,39]

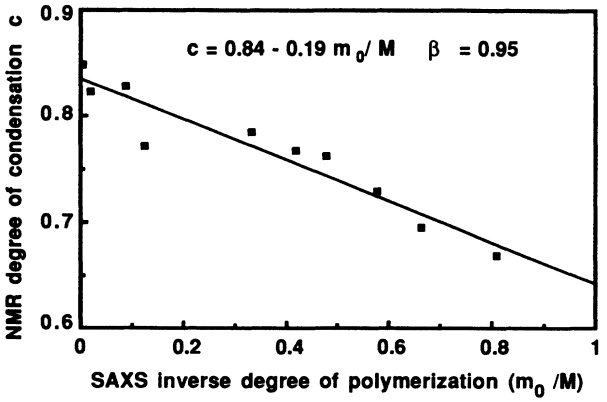

FIG. 8. NMR condensation rate of TEOS vs the reciprocal mass m_0/M obtained by SAXS experiment [β is the correlation coefficient of the fit of the data by Eq. (2)].

Equation (1) can be used to analyze the variation of the degree of condensation during the aggregation phase. Actually, assuming aggregation of the previously defined small units made of n silicon atoms and characterized by m_0 and c_0, the relation between the degree of condensation and the degree of polymerization $DP = M/m_0$ is

$$c = c_0 + (2/nf)(1 - m_0/M) . \quad (2)$$

In Fig. 8, the degree of condensation measured by NMR is plotted versus m_0/M as determined from the SAXS experiments through relation (1). A roughly linear correlation is observed, whose fitting by relation (2) yields $c_0 = 0.64$ and $n = 2.6$ with $f = 4$. As shown in the previous section, this value for n is too small to account for the observed degrees of condensation. However, this discrepancy could be removed by taking into account the polydispersity of the aggregates. Actually, the scattering experiments depend on the weight-average mass M_w, while the number-average mass M_n, which is smaller, enters in Eq. (2). Consequently, a revised fit with a smaller value for M would give a larger and more consistent value for n. Unfortunately, we have not at the present time enough information on the mass distribution in our system to perform this correction.

GELATION

The gel time for the studied TEOS solution was 49 days. It is seen in Fig. 3 that there is no discontinuity in

the condensation kinetics at that time and that the degree of condensation continues to increase in the gelled state. We have checked that acidic TEOS solutions with different TEOS:ethanol:water proportions (1:6:10, 1:6:6, and 1:4:4) exhibit exactly the same structure at t_g (q_2:q_3:q_4 = 10:55:35), whatever the value of t_g is (from 49 to 76 days). This means that our data and their subsequent analysis are representative of alkoxide condensation in the case of rapid and nearly complete hydrolysis.

As recently observed by Vega and Sherer,[40] the main effect of gelation is a progressive broadening of the NMR lines due to a slowing down of the molecular motion, which becomes unable to average the anisotropic chemical shift and the dipolar coupling with the protons. This effect should be distinguished from the broadening arising from the spreading of isotropic chemical shift due to an increasing number of possible surroundings for a silicon nucleus. This difference can be pointed out by comparing static and MAS spectra. Figure 9 shows spectra recorded with and without rotation at $t=t_g$, $1.4t_g$, and $4.1t_g$. MAS spectra show only a small evolution which reflects the slow condensation process. On the other hand, the static spectra display a dramatic broadening due to the progressive freezing of the molecular rotational motion. It is evident from Fig. 9 that this freezing is far from being complete at t_g, implying residual motion at frequencies larger than 1 kHz beyond the gel time. At $t=4.1t_g$ the static spectrum looks like the one which is expected for nonaveraged anisotropic chemical shift powder distribution. At $t=t_g$ and $1.4t_g$, the spectra could be regarded as the superposition of two contributions: a rigid-lattice signal similar to the static spectrum at $t=4.1t_g$ and a motional-narrowed signal similar to the MAS spectrum. The first contribution would correspond to the gel fraction and the second one to the sol fraction. However, an alternative explanation could be to assume a single component spectrum which becomes progressively broadened as the motional narrowing is restricted. Although the spectra shape seems to favor the two-component hypothesis, a definite conclusion cannot be reached before a curve deconvolution has been performed.

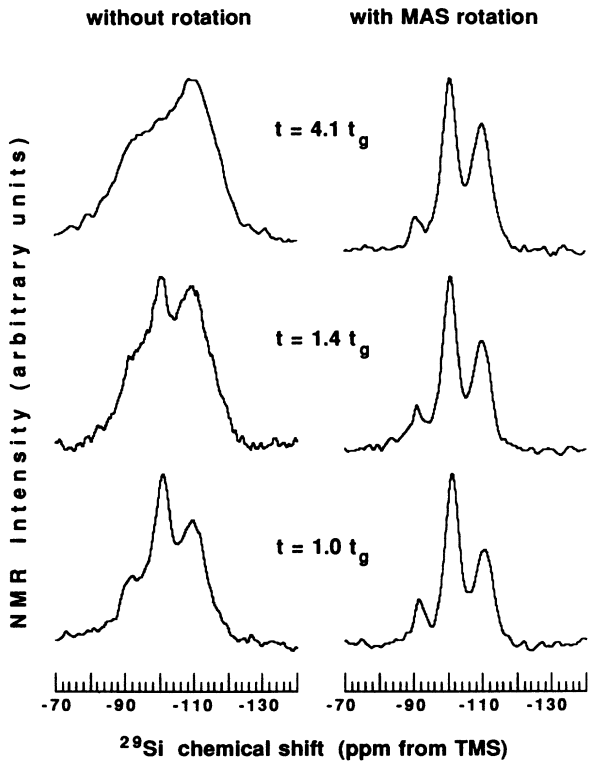

FIG. 9. Comparison of ^{29}Si NMR spectra of condensed TEOS without and with MAS rotation at different times after t_g.

These results are consistent with viewing the gel transition as resulting from the formation of a large-scale percolation cluster (the gel phase), coexisting with smaller aggregates (the sol phase). After t_g, the small clusters are progressively connected to the large one. This leads to a further increase of the condensation rate and to a decrease of the motional-narrowed contribution to the static NMR spectrum. The kinetics of this growing process which results from the formation of bridges between mobile and static units should be different from the kinetics of the free aggregation before t_g. However, it is difficult to characterize them quantitatively by NMR because of the small variation of the degree of condensation in the gelled state: from $c=0.81$ at t_g to $c=0.84$ at $4.1t_g$.

Finally, for $t=t_g$, $1.4t_g$, and $1.7t_g$, we have observed that a gelled sample rotated for a few minutes at 3 kHz goes back to the liquid state. This no longer happens at $t=4.1t_g$. The degree of condensation continues to increase in the recovered liquid state as in the gelled state and the spectra recorded without rotation exhibit a similar broadening. Although the macroscopic viscosity, qualitatively appreciated from the mobility of a bubble in the sample container, increases with time, regelation does not occur for time of the order of t_g. For example, the sample liquified at $t=1.4t_g$ was still in the liquid state five months later. Centrifugation may produce breaking and/or disentangling of the macromolecules. Both are expected to restore the liquid state. However, the only destruction of a fraction of the bonds cannot explain that the gel state is not recovered within a time of the order of t_g and that the NMR spectra show the same broadening as in the gel state. Thus the main effect of the centrifugation should be to unravel the macromolecules. Large clusters with a sufficiently low mobility to give rise to nonaveraged NMR lines subsist, but gelation is inhibited because of the spatial separation of the clusters. This emphasizes the role of the physical entanglement of the aggregates in the achievement of a macroscopic gel state.

CONCLUSION

In conclusion, our data lead to the following picture of the condensation kinetics of rapidly hydrolyzed alkoxides. The first phase, which corresponds to the logarithmic part in the time evolution of the degree of condensation, consists in the progressive assembling of small organized units. For trivalent systems, this ends the con-

densation process because of the lack of remaining available bonds. For tetravalent TEOS, this phase is followed by the growth of fractal clusters, whose kinetics are consistent with reaction limited cluster-cluster aggregation with preferential reactions between peripheral sites. This should lead to moderately polydisperse clusters, intermediate between the strictly monodisperse case of hierarchical aggregation and the strongly polydisperse case of unrestricted RLCA. Gelation, which occurs when the volume fraction occupied by the aggregates becomes of the order of 1, is due to the physical entanglement of the macromolecules, which allows the formation of a large scale percolating cluster. In the gelled state, condensation continues by progressive transformation of the mobile sol phase into the static gel phase.

ACKNOWLEDGMENTS

It is a pleasure to acknowledge illuminating discussions on aggregation mechanisms with M. Kolb. The Laboratoire de Physique de la Matière Condensée is supported by the Centre National de la Recherche Scientifique as Unité de Recherche Associée No. 1254.

[1]B. B. Mandelbrot, *The Fractal Geometry of Nature* (Freeman, San Francisco, 1982).

[2]For recent studies of sol-gel polymerization, see (a) *Better Ceramics Through Chemistry II,* Materials Research Society Symposia Proceedings, edited by C. J. Brinker, D. E. Clark, and D. R. Ulrich (Materials Research Society, Pittsburgh, 1986), Vol. 73; (b) *Better Ceramics Through Chemistry III,* Materials Research Society Symposia Proceedings, edited by C. J. Brinker, D. E. Clark, and D. R. Ulrich (Materials Research Society, Pittsburgh, 1988), Vol. 121.

[3]G. Engelhardt, W. Atlenburg, D. Hoebbel, and W. Wicker, Z. Anorg. Allg. Chem. **428**, 43 (1977).

[4]R. K. Harris and C. T. G. Knight, J. Chem. Soc. D **421**, 726 (1980).

[5]I. Artaki, M. Bradley, T. W. Zerda, and J. Jonas, J. Phys. Chem. **89**, 4399 (1985).

[6]I. Artaki, S. Sinha, A. D. Irwin, and J. Jonas, J. Non-Cryst. Solids **72**, 391 (1985).

[7]G. Orcel and L. Hench, J. Non-Cryst. Solids **79**, 177 (1986).

[8]L. W. Kelts, N. J. Effinger, and S. M. Melpoder, J. Non-Cryst. Solids **83**, 353 (1986).

[9]B. E. Yoldas, J. Non-Cryst. Solids **82**, 11 (1986).

[10]C. C. Lin and J. D. Basil, in Ref. 2(a), p. 585.

[11]J. C. Pouxviel, J. P. Boilot, J. C. Beloeil, and J. Y. Lallemand, J. Non-Cryst. Solids **89**, 345 (1987).

[12]J. C. Pouxviel and J. P. Boilot, J. Non-Cryst. Solids **94**, 374 (1987).

[13]A. H. Boonstra and T. N. M. Bernads, J. Non-Cryst. Solids **108**, 249 (1988).

[14]L. W. Kelts and N. J. Armstrong, J. Mat. Res. **4**, 423 (1989).

[15]D. W. Schaefer and K. D. Keefer, Phys. Rev. Lett. **53**, 1383 (1984).

[16]J. C. Pouxviel, J. P. Boilot, A. Lecomte, and A. Dauger, J. Phys. (Paris) **48**, 921 (1987).

[17]B. Cabane, M. Dubois, and R. Duplessix, J. Phys. (Paris) **48**, 2131 (1987).

[18]J. E. Martin, J. W. Wilcoxon, and D. Adolf, Phys. Rev. A **36**, 1803 (1987).

[19]M. Dubois and B. Cabane, Macromolecules **22**, 2526 (1989).

[20]J. E. Martin and J. P. Wilcoxon, Phys. Rev. A **39**, 252 (1989).

[21]G. Engelhardt and D. Michel, *High Resolution Solid-State NMR of Silicates and Zeolites* (Wiley and Sons, New York, 1987).

[22]R. Aelion, A. Loebel, and F. Eirich, J. Am. Chem. Soc. **72**, 5705 (1950).

[23]K. D. Keefer, Mat. Res. Soc. Symp. Proc. **32**, 15 (1984).

[24]R. K. Iler, *The Chemistry of Silica* (Wiley, New York, 1979), Chap. 3.

[25]C. Okkerse, in *Physical and Chemistry Aspects of Adsorbents and Catalysts,* edited by B. G. Linsen (Academic, New York, 1970), Chap. 5.

[26]E. R. Pohl and F. D. Osterholtz, in *Molecular Characterization of Composite Interfaces,* edited by H. Ishida and G. Kimar (Plenum, New York, 1985), p. 157.

[27]Curves looking like those in Fig. 5 were obtained in a theoretical kinetic study by Kay and Assink, J. Non-Cryst. Solids **104**, 112 (1988). In their case, the curves pictured the equilibrium concentration of nonhydrolyzed species as a function of the water to silicon ratio.

[28]M. G. Voronkov and V. I. Lavrent'yev, Top. Curr. Chem. **102**, 199 (1982).

[29]A. Guinier and G. Fournet, *Small Angle Scattering of X-rays* (Wiley, New York, 1955).

[30]M. Kolb and R. Julien, J. Phys. (Paris) Lett. **45**, L977 (1984).

[31]D. W. Schaefer, J. P. Wilcoxon, K. D. Keefer, B. C. Bunker, R. K. Pearson, I. M. Thomas, and D. E. Miller, in *Physics and Chemistry of Porous Media-II (Schlumberger-Doll Research, Ridgefield, Connecticut, 1986),* Proceedings of the Second International Symposium on the Physics and Chemistry of Porous Media, AIP Conf. Proc. No. 154, edited by Jayanth R. Banavar, Joel Koplik, and Kenneth W. Winkler (AIP, New York, 1986), p. 1.

[32]D. W. Schaefer and K. D. Keefer, in Ref. 2(a), p. 277.

[33]D. W. Schaefer, Science **243**, 1023 (1989).

[34]R. C. Ball, D. A. Weitz, T. A. Witten, and F. Leyvraz, Phys. Rev. Lett. **58**, 274 (1987).

[35]P. Meakin and F. Family, Phys. Rev. A **38**, 2110 (1988).

[36]M. Y. Lin, H. M. Lindsay, D. A. Weitz, R. C. Ball, R. Klein, and P. Meakin, Proc. R. Soc. London, Ser. A **423**, 71 (1989).

[37]M. F. Bechtold, W. Mahler, and R. A. Shunn, J. Polym. Sci. Polym. Chem. Ed. **18**, 2823 (1980).

[38]H. Yang, Z. H. Ding, Z. H. Jiang, and X. P. Xu, J. Non-Cryst. Solids **112**, 449 (1989).

[39]P. G. Van Dongen and M. H. Ernst, Phys. Rev. Lett. **54**, 1396 (1985).

[40]A. J. Vega and G. W. Sherer, J. Non-Cryst. Solids **111**, 153 (1989).